IEEE Access
Multidisciplinary | Rapid Review | Open Access Journal

Received 19 October 2023, accepted 17 November 2023, date of publication 21 November 2023,
date of current version 29 November 2023.

Digital Object Identifier 10.1109/ACCESS.2023.3335170

EXPOSITION

A New Approach to the Analysis of the Compensation Networks of WPT Systems

MANUELE BERTOLUZZO, GIUSEPPE BUJA, (Life Fellow, IEEE), DANIELE DESIDERI, AND AMRITANSH SAGAR, (Senior Member, IEEE)
Department of Industrial Engineering, University of Padua, 35129 Padua, Italy
Corresponding author: Manuele Bertoluzzo (manuele.bertoluzzo@unipd.it)

ABSTRACT The wireless power transfer systems represent a viable solution to make more user friendly the procedure of charging the battery of electric vehicles. The performances of these systems are greatly affected by their compensation networks and are usually studied by considering the first harmonic equivalent circuit of the system. This paper presents a new approach to writing the equations that describe these circuits and expresses them in a form that highlight the contribution of the coupled coils and of their compensation networks. The procedure to obtain the equations is described in details and the equations themselves are analyzed to derive from them the qualitative characteristics of the wireless power transfer system. In the last part of the paper a numerical analysis of a study case is reported, supporting the results by means of simulations.

INDEX TERMS Compensation networks, equivalent circuits, wireless power transmission.

I. INTRODUCTION

A widespread use of electric vehicles is commonly considered as a viable approach to the decrease of the pollutant emissions that are affecting the global climate [1], [2], [3]. Some problems are still hindering the diffusion of such vehicles. One of them is the somewhat unfriendly battery charging procedure, which requires to tamper with cables, plugs, and connectors. This issue can be conveniently bypassed if wireless power transfer systems (WPTSs) are used to charge the battery [4], [5], [6], [7].

The functioning principle of the inductive WPTSs is based on the inductive coupling between two coils and is the same as that of the coreless transformer, with the difference that the performances of the system are greatly enhanced by the use of suitable compensation networks (CNs) [8], [9].

The CNs are passive circuits, formed by inductors and capacitors, inserted between the supply generator of the WPTS and the transmitting coil, and between the receiving coil and the load. Their main functions are to increase the effectiveness and efficiency of the WPTS by minimizing the supply voltage and current needed to transfer to the load a given amount of power [10], [11], [12]. Usually, these effects are achieved by exploiting some form of resonance between the CNs' components themselves and/or between the components and the self-inductances of the coupled coils.

The use of the resonance entails that the WPTSs are in most of cases supplied at a given and fixed frequency. For vehicular applications, the nominal value of the supply frequency is 85 kHz, according to the SAE J2954 standard [13]. Given the constant-frequency operations, it is common to model and analyze the behavior of the WPTSs by considering their first harmonic equivalent circuit [14], [15]. These circuits are not much complex and can be studied using the conventional approaches based, as an example, on the Kirchhoff's laws [15]. Nevertheless, if the CNs are formed by two or more components and the coupled coils are more than two, the equations that describe the system functioning may result involved and it is difficult to recognize the effect of the single WPTS elements on the overall functioning [16], [17].

This paper presents a new approach to writing the mathematical equations that describe the functioning of a WPTS. In particular, the mathematical model of the coupled coils and of the relevant CNs is obtained. Obviously, the resulting

The associate editor coordinating the review of this manuscript and approving it for publication was Derek Abbott.

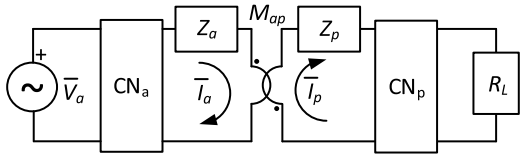

FIGURE 1. Schematic representation of a pickup supplied by one transmitting coil.

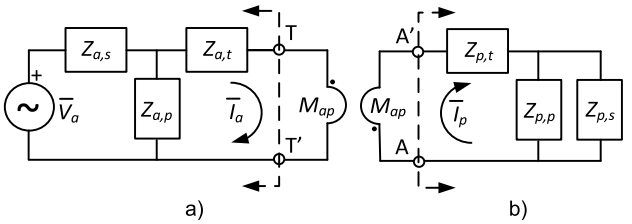

FIGURE 2. General scheme of the CN connected to the transmitting coil (a) and of the CN connected to the pickup (b).

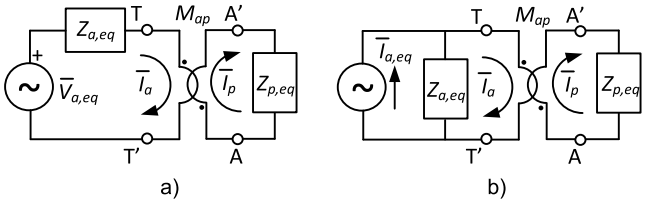

FIGURE 3. Thevenin (a) and Norton (b) equivalent of a pickup supplied by one transmitting coil.

equations are equivalent to those obtained using the classical approach based on Kirchhoff's laws [16], [17], [18]. However, the approach followed in this paper to work out the circuital equations gives two major contributions: 1) the procedure is closely linked to the functioning of the system and to the physical phenomena that take place in it so that the procedure itself constitutes a sort of analysis of the system and gives a deep insight in the phenomena involved in its functioning; 2) the obtained equations have a different layout with respect to those coming from the conventional methods and result "automatically" written in a form that highlights the contribution of the different element of the WPTS, such as the mutual inductances between the coils and the equivalent impedances of the CNs. Therefore, these equations are suitable for the design of the system and for carrying out a "what if" type analysis.

Section II of the paper considers a receiving coil, from here on denoted as "pickup", coupled with only one transmitting coil. General CNs with T topology are considered and the Thevenin and Norton equivalent circuits of the transmitting and the receiving sections of the WPTS are given [19], [20], [21]. From them, the equations that describe this simple WPTS are derived. Section III considers the more general condition of having two transmitting coils that are coupled to the same pickup and derives the complete equations for this arrangement. Section IV demonstrates that the obtained equations are equivalent to those coming from the application of the loops method based on the second Kirchhoff's law. Section V analyzes the equations obtained in Section III and draws some considerations regarding the WPTS functioning. Section VI applies the equations to the analysis of a particular study case and compares the obtained numerical results with those coming from circuital simulations. Section VII concludes the paper. Appendix reports the complete equations worked out in Section III.

II. PICKUP SUPPLIED BY ONE COIL

A pickup supplied by only one transmitting coil is schematized in Fig. 1. The transmitting coil "a" is represented by its impedance Z_a and by its mutual inductance with the pickup, denoted as M_{ap}. The coil is supplied by a sinusoidal voltage generator, represented by the phasor $\bar{V}_a$, through the compensation network CN_a. The current $\bar{I}_a$ flowing in the coil induces a voltage across the pickup that, in turn, forces the circulation of the current $\bar{I}_p$ through the pickup. The latter one is represented by its impedance Z_p and its mutual inductance with the transmitting coil. The pickup is connected to the load through the compensation network CN_p. The load is constituted by the cascade of a rectifier, a battery charger and the battery. These elements absorb only active power and, hence, can be represented by the equivalent resistor R_L. The actual value of R_L changes with the state of charge of the battery, but its variation does not affect the mathematical expressions obtained in the subsequent Sections.

A large number of different topologies have been proposed for the CNs in order to meet different requirements of the WPTS functioning. Most of them can be reduced to the general schemes of Fig. 2a, for the transmitting coil, and of Fig. 2b for the pickup. In Fig. 2a, $Z_{a,t}$ accounts also for the transmitting coil's impedance whilst in Fig. 2b $Z_{p,t}$ accounts also for the pickup impedance and $Z_{p,s}$ accounts also for the equivalent load R_L.

The circuit seen from the terminals T-T' of Fig. 2a, formed by the voltage generator and CN_a, can be represented by its Thevenin equivalent circuit redrawing the scheme of Fig. 2 as in Fig. 3a [19], [20]. The equivalent voltage generator and impedance are expressed by (1) and (2).

$$\bar{V}_{a,eq} = \bar{V}_a \frac{Z_{a,p}}{Z_{a,s} + Z_{a,p}} \tag{1}$$

$$Z_{a,eq} = \frac{Z_{a,s} Z_{a,p}}{Z_{a,s} + Z_{a,p}} + Z_{a,t} \tag{2}$$

The equivalent impedance $Z_{p,eq}$ seen from the terminals A-A' of Fig. 2b is given by an expression similar to (2), provided that the subscript "a" is substituted for by "p".

It is also possible to use the Norton equivalent circuits of the schemes of Fig. 2, obtaining Fig. 3b, where $Z_{a,eq}$ is still given by (2) and $\bar{I}_{a,eq}$ is equal to

$$\bar{I}_{a,eq} = \bar{V}_a \frac{Z_{a,p}}{Z_{a,s} Z_{a,p} + Z_{a,s} Z_{a,t} + Z_{a,p} Z_{a,t}} \tag{3}$$

TABLE 1. Equivalent generators and impedances.

Topology	$\bar{V}_{a,eq}$	$\bar{I}_{a,eq}$	$Z_{a,eq}$
Series	$\bar{V}_a$	∞	0
Parallel	$\bar{V}_a$	$\frac{\bar{V}_a}{Z_{a,t}}$	$Z_{a,t}$
LCL (a) $(Z_{a,s} = -Z_{a,p})$	∞	$\frac{\bar{V}_a}{Z_{a,s}}$	∞
LCL (b) $(Z_{a,t} = -Z_{a,p})$	$\frac{\bar{V}_a Z_{a,p}}{Z_{a,s} + Z_{a,p}}$	$-\frac{\bar{V}_a}{Z_{a,p}}$	$-\frac{{Z_{a,p}}^2}{Z_{a,s} + Z_{a,p}}$
LCL (c) $(Z_{a,p} = -Z_{a,s} \parallel Z_{a,t})$	$\frac{\bar{V}_a Z_{a,p}}{Z_{a,s} + Z_{a,p}}$	∞	0

Inserting in (1)-(3) the actual impedances of the CNs it is possible to work out the equivalent circuit of the transmitting section of the WPT considering different CNs. As an example, setting $Z_{a,t} = Z_a$ (i.e. no impedance is connected in series to the coil "a"), $Z_{a,s}$=-Z_a, and $Z_{a,p} = \infty$, the series compensation of the transmitting coil inductance is obtained. Otherwise, setting $Z_{a,t} = Z_a$, $Z_{a,s}$=*0*, and $Z_{a,p}$=-Z_a, the parallel compensation is implemented. Tab. 1 has been obtained applying (1)-(3) to different topologies of CNs and different types of resonance. In working out the results, only the reactive components of the impedances have been considered whilst the parasitic resistances of the coils and of the components of the CNs have been disregarded. This approach is usually followed in the first step of the CNs design. A more detailed analysis requires to account for the effect of the parasitic resistances of the inductors and of the capacitors that constitute the CNs. In this case, $Z_{a,s}$, $Z_{a,p}$, $Z_{a,t}$, and the other impedances of the CNs become complex quantity instead of imaginary ones. Nevertheless, (1)-(3) and all the subsequent mathematical results are still correct.

It is worth to highlight that even if the transmitting coil is supplied by a voltage generator, a proper selection of CN_a makes it appear as being supplied by a current generator, as it happens in the case of the LCL topology denoted with (a), where $Z_{a,s}$ resonates with $Z_{a,p}$. In this case, the Thevenin equivalent circuit is not defined because the denominator of (1) is equal to 0. However, it is possible to define the Norton equivalent circuit. It is formed only by an ideal current generator because $Z_{a,eq}$ results infinite whilst (3) gives a finite result.

When the Thevenin equivalent circuit is considered, the equations that link the currents flowing in the transmitting coil and in the pickup to the supply voltage are

$$\begin{cases} \bar{V}_{a,eq} - Z_{a,eq}\bar{I}_a - j\omega M_{ap}\bar{I}_p = 0 \\ -j\omega M_{ap}\bar{I}_a - Z_{p,eq}\bar{I}_p = 0 \end{cases} \tag{4}$$

From them, the currents are readily derived as

$$\begin{cases} \bar{I}_a = \bar{V}_{a,eq}\dfrac{1}{z_{a,eq} + \frac{\omega^2 M_{ap}^2}{z_{p,eq}}} \\ \bar{I}_p = -\dfrac{j\omega M_{ap}}{z_{a,eq}}\bar{V}_{a,eq}\dfrac{1}{z_{p,eq} + \frac{\omega^2 M_{ap^2}}{z_{a,eq}}} \end{cases} \tag{5}$$

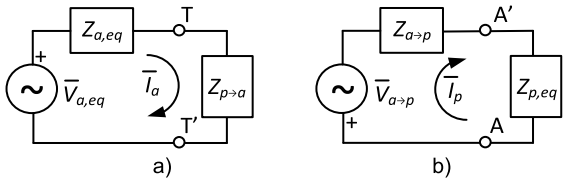

FIGURE 4. Receiving side Thevenin equivalent circuit reflected to the transmitting side (a) and transmitting side Thevenin equivalent circuit reflected to the receiving side (b).

The first of (5) confirms the well-known results by which the pickup is seen from the terminals T-T' as the reflected impedance

$$Z_{p\to a} = \frac{\omega^2 M_{ap}^2}{Z_{p,eq}} \tag{6}$$

connected in series to the transmitting coil.

The second of (5) states that looking from the terminals A and A', the voltage generator, the CN_a and the transmitting coil are seen as an equivalent generator having open circuit voltage $\bar{V}_{a\to p}$ and internal resistance $Z_{a\to p}$ given by

$$\bar{V}_{a\to p} = \frac{j\omega M_{ap}}{Z_{a,eq}}\bar{V}_{a,eq} \tag{7}$$

$$Z_{a\to p} = \frac{\omega^2 M_{ap}^2}{Z_{a,eq}}. \tag{8}$$

Equations (5)-(8) are conveniently represented by the schemes drawn in Fig. 4.

If the Norton equivalent circuit is considered, the second of (4) is still valid while the first of them must be substituted for by

$$\bar{I}_{a,eq} - \frac{j\omega M_{ap}}{Z_{a,eq}}\bar{I}_p - \bar{I}_a = 0. \tag{9}$$

The currents $\bar{I}_a$ and $\bar{I}_p$ are now given by

$$\begin{cases} \bar{I}_a = \bar{I}_{a,eq}\dfrac{z_{a,eq}}{z_{a,eq} + \frac{\omega^2 M_{ap}^2}{z_{p,eq}}} \\ \bar{I}_p = \bar{I}_{a,eq}\dfrac{z_{a,eq}}{j\omega M_{ap}}\dfrac{\frac{\omega^2 M_{ap^2}}{z_{a,eq}}}{z_{p,eq} + \frac{\omega^2 M_{ap}^2}{z_{a,eq}}}. \end{cases} \tag{10}$$

Equations (10) represents the functioning of the circuits drawn in Fig. 5, thus it can be concluded that the receiving side is still seen as the reflected impedance (6) while the equivalent current generator representing the transmitting side of the WPTS has the internal impedance given by (8) and the short circuit current $\bar{I}_{a\to p}$ given by (11)

$$\bar{I}_{a\to p} = -\bar{I}_{a,eq}\frac{Z_{a,eq}}{j\omega M_{ap}}. \tag{11}$$

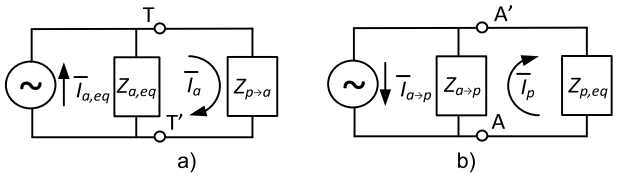

FIGURE 5. Receiving side Norton equivalent circuit reflected to the transmitting side (a) and transmitting side Norton equivalent circuit reflected to the receiving side (b).

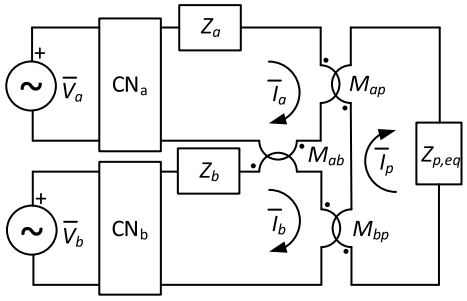

FIGURE 6. Schematic representation of WPTS with a pickup coupled to two transmitting coils.

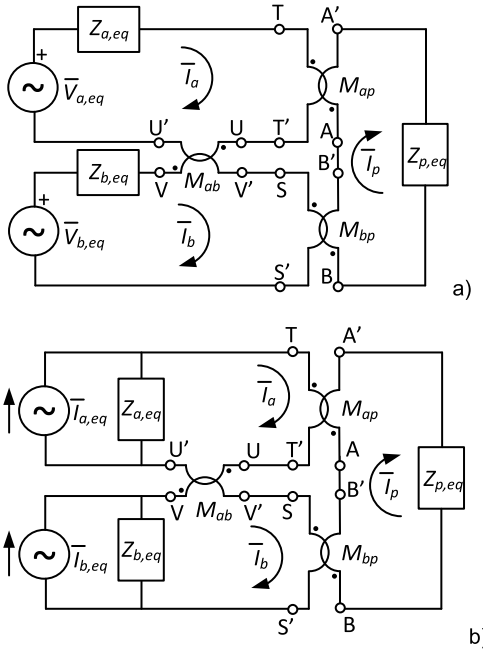

FIGURE 7. Schematic representation of a WPTS with a pickup coupled to two transmitting coils using the Thevenin (a) and the Norton (b) equivalent circuits.

III. PICKUP SUPPLIED BY TWO COILS

The condition of a pickup coupled at the same time with two transmitting coils, denoted as "a" and "b" is schematized in Fig. 6. Besides by their impedances Z_a and Z_b, the transmitting coils are characterized by their mutual inductance M_{ab} and by the mutual inductances M_{ap} and M_{bp} between each of them and the pickup.

Generally speaking, it is possible that the two transmitting coils and their CNs are different, and that M_{ap} and M_{bp} are different as well. The only limitation assumed in this paper is that both the CNs can be represented by equivalent circuits with the same topology, either Thevenin or Norton.

By considering the equivalent circuits of Fig. 3, the scheme of the WPTS with two transmitting coils and one pickup can be redrawn as in Fig. 7a or Fig. 7b.

A. CNs WITH THEVENIN EQUIVALENT CIRCUIT

If both CN_a and CN_b are be represented by means of Thevenin equivalent circuits, the scheme of Fig. 7a is considered. The analysis of the circuit is performed by exploiting the principle of the superposition of the effects setting $\bar{V}_b = 0$, so that, by (1) it is $\bar{V}_{b,eq} = 0$.

1) RELATION BETWEEN $\bar{I}_a$ AND $\bar{V}_{a,eq}$

The first step in the circuit solution consists in working out $\bar{I}_a$ solving the loop relevant to the transmitting coil "a". This is done by reflecting across the terminals T-T' the effect of the coil couplings due to M_{ab} and M_{bp} and across the terminals U-U' the effects due to M_{ap} and M_{bp}.

Given that $\bar{V}_{b,eq} = 0$, the scheme of Fig. 7a can be redrawn in the form of Fig. 8a, where $\bar{V}_{ab,ind}$, given by (12) is the voltage induced across V-V' by the current $\bar{I}_a$.

$$\bar{V}_{ab,ind} = j\omega M_{ab}\bar{I}_a. \tag{12}$$

The block denoted with V,Z accounts for the voltage and the impedance reflected across the terminals U-U' through the coupling due to M_{ab}. These quantities will be considered in the next paragraphs.

By applying (7) and (8) to $\bar{V}_{ab,ind}$ and $Z_{b,eq}$, the voltage and the impedance of the loop relevant to $\bar{I}_b$ are reflected to the receiving side as shown in Fig. 8b and according to

$$\bar{V}_{b\to p} = -\frac{j\omega M_{bp}}{Z_{b,eq}}\bar{V}_{ab,ind} = \frac{\omega^2 M_{bp}M_{ab}}{Z_{b,eq}}\bar{I}_a \tag{13}$$

$$Z_{b\to p} = \frac{\omega^2 M_{bp}^2}{Z_{b,eq}}. \tag{14}$$

The minus sign in the first of (13) originates because, in comparison with Fig 3a, from where (7) has been obtained, the polarity of $\bar{V}_{ab,ind}$ is opposite to that of $\bar{V}_{a,eq}$. This condition will appear again in the following discussion.

Applying (7) and (8) to the loop relevant to $\bar{I}_p$, the receiving side voltage and impedance reflected across the terminals T and T' through the coupling M_{ap} result in

$$\bar{V}_{p\to a} = -\frac{j\omega M_{ap}}{Z_{p,eq}+Z_{b\to p}}\bar{V}_{b\to p} = -\frac{j\omega^3 M_{bp}M_{ab}M_{ap}}{Z_{p,eq}Z_{b,eq}+\omega^2 M_{bp}^2}\bar{I}_a \tag{15}$$

$$Z_{p\to a} = \frac{\omega^2 M_{ap}^2}{Z_{p,eq}+Z_{b\to p}} = \frac{\omega^2 M_{ap}^2}{Z_{p,eq}+\frac{\omega^2 M_{bp}^2}{Z_{b,eq}}}, \tag{16}$$

as modelled in Fig. 8c.

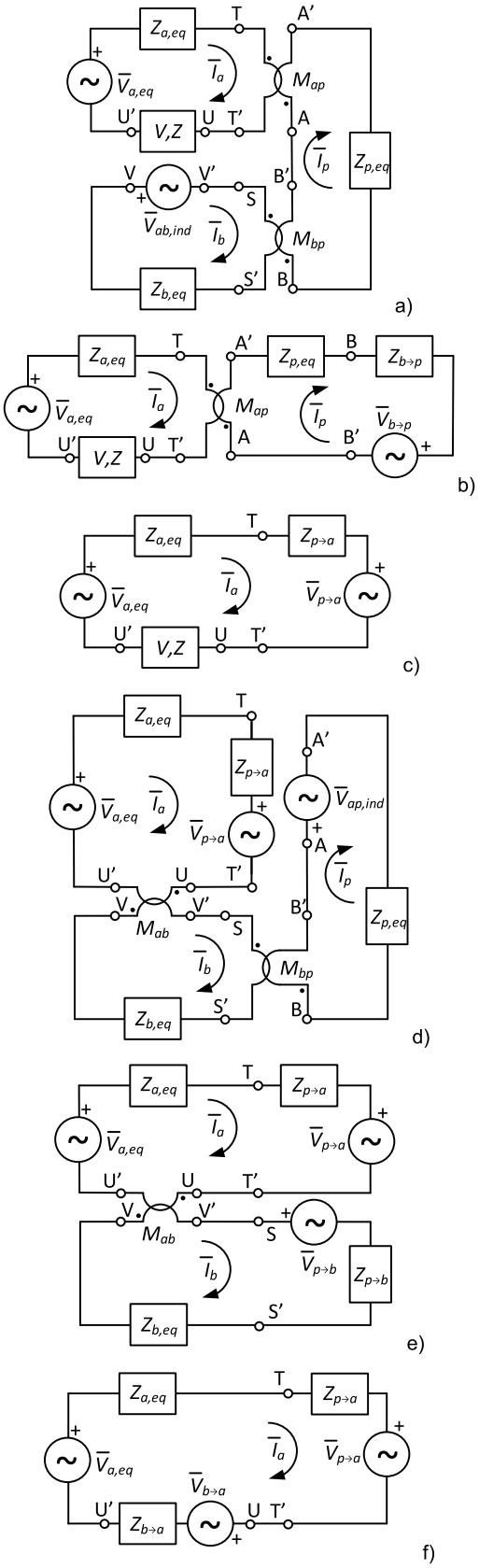

FIGURE 8. Subsequent equivalent circuits used to reflect the loops relevant to coil "b" and the pickup to the loop relevant to the coil "a".

The procedure to find out the equivalent voltage and impedance of the block V,Z begins by redrawing the WPTS scheme as in Fig. 8d. The figure derives directly from Fig. 7a, represents the effects of the pickup on the transmitting coil "a" using (15) and (16), and accounts for the effects of the coil "a" on the pickup through the induced voltage $\bar{V}_{ap,ind}$ given by

$$\bar{V}_{ap,ind} = j\omega M_{ap}\bar{I}_a. \tag{17}$$

The receiving side voltage and impedance are reflected across the terminals S-S' by using again (7) and (8) obtaining

$$\bar{V}_{p\to b} = -\frac{j\omega M_{bp}}{Z_{p,eq}}\bar{V}_{ap,ind} = \frac{\omega^2 M_{bp}M_{ap}}{Z_{p,eq}}\bar{I}_a \tag{18}$$

$$Z_{p\to b} = \frac{\omega^2 M_{bp}^2}{Z_{p,eq}}, \tag{19}$$

as shown in Fig. 8e.

The voltage and the impedance of the loop relevant to coil "b" are reflected across the terminals U-U' as shown in Fig. 8f, finding the exact model of the block V,Z given by (20) and (21).

$$\bar{V}_{b\to a} = -\frac{j\omega M_{ab}}{Z_{b,eq}+Z_{p\to b}}\bar{V}_{p\to b} = -\frac{j\omega^3 M_{ab}M_{bp}M_{ap}}{Z_{p,eq}Z_{b,eq}+\omega^2 M_{bp}^2}\bar{I}_a \tag{20}$$

$$Z_{b\to a} = \frac{\omega^2 M_{ab}^2}{Z_{b,eq}+Z_{p\to b}} = \frac{\omega^2 M_{ab}^2}{Z_{b,eq}+\frac{\omega^2 M_{bp}^2}{Z_{p,eq}}}. \tag{21}$$

Finally, by inspection of Fig. 8f, the expression that links $\bar{I}_a$ to $\bar{V}_{a,eq}$ is obtained in the form

$$\bar{V}_{a,eq} - \bar{V}_{b\to a} - \bar{V}_{p\to a} = \left(Z_{a,eq} + Z_{b\to a} + Z_{p\to a}\right)\bar{I}_a. \tag{22}$$

By using (15), (16), (20), (21) it is rewritten as (A1), reported in the appendix.

2) RELATION BETWEEN $\bar{I}_b$ AND $\bar{V}_{a,eq}$

The procedure to find out the relation that links $\bar{I}_b$ and $\bar{V}_{a,eq}$ is similar to that one described in the previous subsection and begins by expressing the voltage induced by $\bar{I}_b$ across the terminals U-U' as

$$\bar{V}_{ba,ind} = j\omega M_{ab}\bar{I}_b. \tag{23}$$

Applying (7) and (8) to the loop relevant to $\bar{I}_a$, the voltage and the impedance reflected across the terminals A-A' of the pickup result

$$\bar{V}_{a\to p} = \frac{j\omega M_{ap}}{Z_{a,eq}}\left(\bar{V}_{a,eq} - \bar{V}_{ba,ind}\right) \tag{24}$$

$$Z_{a\to p} = \frac{\omega^2 M_{ap}^2}{Z_{a,eq}}. \tag{25}$$

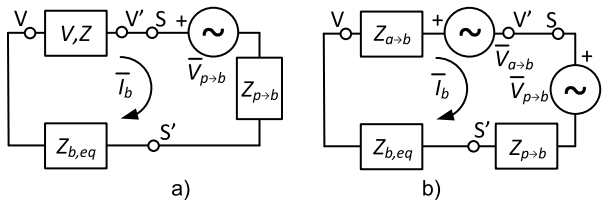

FIGURE 9. Equivalent circuit of the WPTS with two coils and one pickup reflected to the coil "b".

Application of (7) and (8) to the loop relevant to $\bar{I}_p$ gives the voltage and the impedance reflected across the terminals S-S' of the coil "b" obtaining

$$\bar{V}_{p\to b} = -\frac{j\omega M_{bp}}{Z_{p,eq} + \frac{\omega^2 M_{ap}^2}{Z_{a,eq}}} \bar{V}_{a\to p} \tag{26}$$

$$Z_{p\to b} = \frac{\omega^2 M_{bp}^2}{Z_{p,eq} + \frac{\omega^2 M_{ap}^2}{Z_{a,eq}}}. \tag{27}$$

Following from the previous considerations and from (26) and (27), the loop relevant to coil "b" can be represented as in Fig. 9a, using also in this case the block V,Z to represent the effects of the loop relevant to coil "a" across the terminals V-V' of coil "b".

The voltage induced by $\bar{I}_b$ on the pickup is

$$\bar{V}_{bp,ind} = j\omega M_{bp} \bar{I}_b. \tag{28}$$

Together with $Z_{p,eq}$, it is reflected to the loop relevant to $\bar{I}_a$ obtaining

$$\bar{V}_{p\to a} = -\frac{j\omega M_{ap}}{Z_{p,eq}} \bar{V}_{bp,ind} = \frac{\omega^2 M_{ap} M_{bp}}{Z_{p,eq}} \bar{I}_b \tag{29}$$

$$Z_{p\to a} = \frac{\omega^2 M_{ap}^2}{Z_{p,eq}}. \tag{30}$$

On its turn, coil "a" reflects across the terminals V-V' of coil "b" the voltage and the impedance given by

$$\bar{V}_{a\to b} = \frac{j\omega M_{ab}}{Z_{a,eq} + \frac{\omega^2 M_{ap}^2}{Z_{p,eq}}} \left(\bar{V}_{a,eq} - \bar{V}_{p\to a}\right) \tag{31}$$

$$Z_{a\to b} = \frac{\omega^2 M_{ab}^2}{Z_{a,eq} + \frac{\omega^2 M_{ap}^2}{Z_{p,eq}}}, \tag{32}$$

which correspond to the V,Z block of Fig. 9a.

Considering (26), (27), (31), and (32), the loop relevant to coil "b" can be schematized as in Fig. 9b, from which the relation between $\bar{I}_b$ and $\bar{V}_{a,eq}$ is obtained as

$$\bar{V}_{a\to b} + \bar{V}_{p\to b} = -\left(Z_{b,eq} + Z_{a\to b} + Z_{p\to b}\right) \bar{I}_b. \tag{33}$$

The expanded version of (33) is given by (A2).

3) RELATION BETWEEN $\bar{I}_p$ AND $\bar{V}_{a,eq}$

The procedure to find out the relation that links $\bar{I}_p$ to $\bar{V}_{a,eq}$ begins by expressing the voltage induced by $\bar{I}_p$ by across the terminals T-T' as

$$\bar{V}_{pa,ind} = j\omega M_{ap} \bar{I}_p. \tag{34}$$

The voltage generator and the impedance of the loop relevant to $\bar{I}_a$ are reflected across the terminals V-V' of coil "b" obtaining

$$\bar{V}_{a\to b} = \frac{j\omega M_{ab}}{Z_{a,eq}} \left(\bar{V}_{a,eq} - \bar{V}_{pa,ind}\right) \tag{35}$$

$$Z_{a\to b} = \frac{\omega^2 M_{ab}^2}{Z_{a,eq}}. \tag{36}$$

On their turn, the equivalent voltage generator and the impedance of the loop relevant to $\bar{I}_b$ are reflected across the terminals B-B' of the pickup according to

$$\bar{V}_{b\to p} = -\frac{j\omega M_{bp}}{Z_{b,eq} + Z_{a\to b}} \bar{V}_{a\to b} \tag{37}$$

$$Z_{b\to p} = \frac{\omega^2 M_{bp}^2}{Z_{b,eq} + Z_{a\to b}}. \tag{38}$$

In a symmetrical way, the current $\bar{I}_p$ induces across the terminals S-S' the voltage

$$\bar{V}_{pb,ind} = j\omega M_{bp} \bar{I}_p. \tag{39}$$

The latter one and the impedance $Z_{b,eq}$ are reflected by (7) and (8) across the terminals U-U' obtaining

$$\bar{V}_{b\to a} = -\frac{j\omega M_{ab}}{Z_{b,eq}} \bar{V}_{pb,ind} = \frac{\omega^2 M_{ab} M_{bp}}{Z_{b,eq}} \bar{I}_p \tag{40}$$

$$Z_{b\to a} = \frac{\omega^2 M_{ab}^2}{Z_{b,eq}}. \tag{41}$$

The equivalent voltage generator and the impedance of the loop relevant to $\bar{I}_a$ are finally reflected to the pickup by

$$\bar{V}_{a\to p} = \frac{j\omega M_{ap}}{Z_{a,eq} + Z_{b\to a}} \left(\bar{V}_{a,eq} - \bar{V}_{b\to a}\right) \tag{42}$$

$$Z_{a\to p} = \frac{\omega^2 M_{ap}^2}{Z_{a,eq} + Z_{b\to a}}. \tag{43}$$

Considering (35)-(38) and (40)-(43), the loop relevant to the pickup can be schematized as in Fig. 10 and the relation that links $\bar{I}_p$ and $\bar{V}_{a,eq}$ results in

$$\bar{V}_{a\to p} + \bar{V}_{b\to p} = -\left(Z_{p,eq} + Z_{a\to p} + Z_{b\to p}\right) \bar{I}_p. \tag{44}$$

The expanded version of (44) is given by (A3).

4) COILS AND PICKUP CURRENTS WHEN BOTH THE COILS ARE SUPPLIED

The analysis of the circuit functioning when $\bar{V}_{a,eq} = 0$ and only the coil "b" is supplied is performed following the same approach described in the previous subsections. By exploiting the symmetry of the circuit, the relations between the voltage $\bar{V}_{b,eq}$ and the currents in the transmitting coils and in the

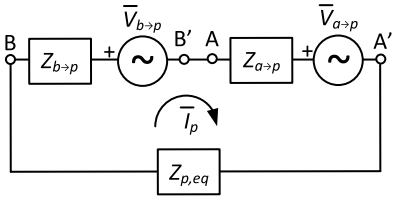

FIGURE 10. Equivalent circuit of the WPTS with two coils and one pickup reflected to the pickup.

pickup are readily derived from (A1)-(A3) and are given by (A4)-(A6).

The terms that multiply the currents on the right-hand side of the pairs of equations (A1)-(A5), (A2)-(A4), and (A3)-(A6) are equal. They have the dimension of an impedance and in (45), (46) and (47) are denoted with $Z_{a,a}$, $Z_{b,b}$, and $Z_{ab,p}$, respectively.

$$Z_{a,a} \triangleq Z_{a,eq} + \frac{\omega^2 M_{ab}^2}{Z_{b,eq} + \frac{\omega^2 M_{bp}^2}{Z_{p,eq}}} + \frac{\omega^2 M_{ap}^2}{Z_{p,eq} + \frac{\omega^2 M_{bp}^2}{Z_{b,eq}}} - 2\frac{j\omega^3 M_{ab} M_{bp} M_{ap}}{Z_{p,eq} Z_{b,eq} + \omega^2 M_{bp}^2} \tag{45}$$

$$Z_{b,b} \triangleq Z_{b,eq} + \frac{\omega^2 M_{ab}^2}{Z_{a,eq} + \frac{\omega^2 M_{ap}^2}{Z_{p,eq}}} + \frac{\omega^2 M_{bp}^2}{Z_{p,eq} + \frac{\omega^2 M_{ap}^2}{Z_{a,eq}}} - 2\frac{j\omega^3 M_{ab} M_{bp} M_{ap}}{Z_{p,eq} Z_{a,eq} + \omega^2 M_{ap}^2}. \tag{46}$$

$$Z_{ab,p} \triangleq Z_{p,eq} + \frac{\omega^2 M_{ap}^2}{Z_{a,eq} + \frac{\omega^2 M_{ab}^2}{Z_{b,eq}}} + \frac{\omega^2 M_{bp}^2}{Z_{b,eq} + \frac{\omega^2 M_{ab}^2}{Z_{a,eq}}} - 2\frac{j\omega^3 M_{ab} M_{bp} M_{ap}}{Z_{a,eq} Z_{b,eq} + \omega^2 M_{ab}^2}. \tag{47}$$

The gains that multiply the voltages on the left-hand side of (A2), (A3), (A4), (A6) are denoted with $K_{a,b}$, $K_{b,a}$, $K_{a,p}$, and $K_{b,p}$. They are given by

$$K_{b,a} \triangleq -\frac{j\omega M_{ab} Z_{p,eq} + \omega^2 M_{bp} M_{ap}}{Z_{p,eq} Z_{b,eq} + \omega^2 M_{bp}^2} \tag{48}$$

$$K_{a,b} \triangleq -\frac{j\omega M_{ab} Z_{p,eq} + \omega^2 M_{bp} M_{ap}}{Z_{p,eq} Z_{a,eq} + \omega^2 M_{ap}^2} \tag{49}$$

$$K_{a,p} \triangleq -\frac{j\omega M_{ap} Z_{b,eq} + \omega^2 M_{bp} M_{ab}}{Z_{a,eq} Z_{b,eq} + \omega^2 M_{ab}^2} \tag{50}$$

$$K_{b,p} \triangleq -\frac{j\omega M_{bp} Z_{a,eq} + \omega^2 M_{ap} M_{ab}}{Z_{a,eq} Z_{b,eq} + \omega^2 M_{ab}^2}. \tag{51}$$

Given these definitions, the currents flowing in the coils and in the pickup when both the supply voltages are applied can be expressed in the form

$$\bar{I}_a = \frac{\bar{V}_{a,eq} + \bar{V}_{b,eq} K_{b,a}}{Z_{a,a}} \tag{52}$$

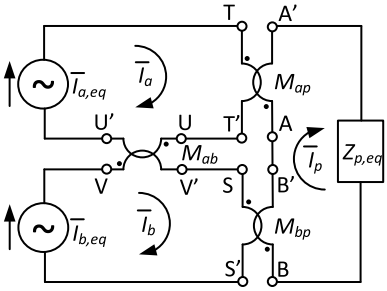

FIGURE 11. Schematic representation of a pickup supplied by two transmitting coils using the Norton equivalent circuit with $Z_{a,eq} = \infty$.

$$\bar{I}_b = \frac{\bar{V}_{a,eq} K_{a,b} + \bar{V}_{b,eq}}{Z_{b,b}} \tag{53}$$

$$\bar{I}_p = \frac{\bar{V}_{a,eq} K_{a,p} + \bar{V}_{b,eq} K_{b,p}}{Z_{ab,p}}. \tag{54}$$

The correctness of the expressions obtained for the three currents can be checked by comparing them with the results coming from the conventional methods used for the circuit solutions, as described in subsequent Section.

B. CNs WITH NORTON EQUIVALENT CIRCUIT

According to Tab. 1, the use of the Norton equivalent circuits is compulsory when $\bar{V}_{a,eq} = \infty$, $Z_{a,eq} = \infty$, $\bar{V}_{b,eq} = \infty$, and $Z_{b,eq} = \infty$. The scheme of Fig. 7b is then simplified in that one reported in Fig. 11, which can be easily solved obtaining the expressions

$$\bar{I}_a = \bar{I}_{a,eq} \tag{55}$$

$$\bar{I}_b = \bar{I}_{b,eq} \tag{56}$$

$$\bar{I}_p = -\frac{j\omega M_{ap} \bar{I}_{a,eq} + j\omega M_{bp} \bar{I}_{b,eq}}{Z_{p,eq}}. \tag{57}$$

IV. CIRCUITAL EQUATIONS OBTAINED USING THE 2ND KIRCHHOFF LAW

The equations that describe the functioning of the circuit represented in Fig. 7a can be obtained applying the second Kirchhoff's law to the loops relevant to the two transmitting coils and the pickup.

By supposing that $\bar{V}_{a,eq} \neq 0$ and $\bar{V}_{b,eq} = 0$, the three voltage equations can be written in matrixial form as

$$\begin{bmatrix} Z_{a,eq} & j\omega M_{ab} & j\omega M_{ap} \\ j\omega M_{ab} & Z_{b,eq} & j\omega M_{bp} \\ j\omega M_{ap} & j\omega M_{bp} & Z_{p,eq} \end{bmatrix} \begin{bmatrix} \bar{I}_a \\ \bar{I}_b \\ \bar{I}_q \end{bmatrix} = \begin{bmatrix} \bar{V}_{a,eq} \\ 0 \\ 0 \end{bmatrix}. \tag{58}$$

The expressions of the three currents as functions of $\bar{V}_{a,eq}$ are readily obtained by inversion of the parameter's matrix. They are given by

$$\bar{I}_a = \frac{Z_{b,eq} Z_{p,eq} + \omega^2 M_{bp}^2}{\Delta} \bar{V}_{a,eq} \tag{59}$$

$$\bar{I}_b = -\frac{j\omega M_{ab} Z_{p,eq} + \omega^2 M_{ap} M_{bp}}{\Delta} \bar{V}_{a,eq} \tag{60}$$

TABLE 2. Prototype parameters.

Parameter	Symbol	Value
Coil "a" self-inductance	L_a	139 μH
Coil "b" self-inductance	L_b	167 μH
Pickup self-inductance	L_p	134 μH
Coil "a" – Coil "b" mutual inductance	M_{ab}	70 μH
Coil "a" – Pickup mutual inductance	M_{ap}	39 μH
Coil "b" – Pickup mutual inductance	M_{bp}	39 μH
Supply angular frequency	ω	$5.34{\cdot}10^5$rad/s
Quality factor	Q	300
Load equivalent resistance	R_L	5.6 Ω
Nominal Power	P_N	1.5 kW

$$\bar{I}_q = -\frac{j\omega M_{ap} Z_{b,eq} + \omega^2 M_{ab} M_{bp}}{\Delta} \bar{V}_{a,eq}, \tag{61}$$

where Δ is the determinant of the matrix, equal to

$$\Delta = Z_{a,eq} Z_{b,eq} Z_{p,eq} + Z_{a,eq}\omega^2 M_{bp}^2 + Z_{b,eq}\omega^2 M_{ap}^2 + + Z_{p,eq}\omega^2 M_{ab}^2 - 2j\omega^3 M_{ab} M_{ap} M_{bp}. \tag{62}$$

The equations (59)-(61) can be reduced to the layout of (A1)-(A3) by simple mathematical manipulations. In the case of (59), the term $\left(Z_{\mathrm{b,eq}} Z_{\mathrm{q,eq}} + \omega^2 M_{bp}^2\right)$ must be collected as common factor at the numerator and the denominator obtaining

$$\bar{I}_a = \frac{\bar{V}_{a,eq}}{Z_{a,eq} + \frac{Z_{b,eq}\omega^2 M_{ap}^2}{Z_{b,eq} Z_{p,eq} + \omega^2 M_{bp}^2} + \frac{Z_{p,eq}\omega^2 M_{ab}^2}{Z_{b,eq} Z_{p,eq} + \omega^2 M_{bp}^2} - \frac{2j\omega^3 M_{ab} M_{ap} M_{bp}}{Z_{b,eq} Z_{p,eq} + \omega^2 M_{bp}^2}}. \tag{63}$$

Then, $Z_{b,eq}$ is collected as common factor of the denominator of the second term of the denominator of (63) and $Z_{p,eq}$ is collected as common factor of the denominator of the third term of the denominator of (63). After the simplification, the expression of $\bar{I}_{a,eq}$ results in

$$\bar{I}_a = \frac{\bar{V}_{a,eq}}{Z_{a,eq} + \frac{\omega^2 M_{ap}^2}{Z_{p,eq} + \frac{\omega^2 M_{bp}^2}{Z_{b,eq}}} + \frac{\omega^2 M_{ab}^2}{Z_{b,eq} + \frac{\omega^2 M_{bp}^2}{Z_{p,eq}}} - \frac{2j\omega^3 M_{ab} M_{ap} M_{bp}}{Z_{b,eq} Z_{p,eq} + \omega^2 M_{bp}^2}}, \tag{64}$$

which is equivalent to (A1)

The manipulations needed to reduce (60) to (A2) and (61) to (A3) are quite similar. The first of them starts by collecting the term $\left(j\omega M_{ab} Z_{p,eq} + \omega^2 M_{bp} M_{ap}\right)$ whilst the second one begins by collecting the term $\left(j\omega M_{ap} Z_{b,eq} + \omega^2 M_{bp} M_{ab}\right)$.

Equations (A4)-(A6) can be derived by the same process described above but setting that $\bar{V}_{a,eq} = 0$ and $\bar{V}_{b,eq} \neq 0$.

It is worth emphasizing that the procedure followed to obtain (A1)-(A3) from (59)-(61), even if simple in its application, is not trivial unless the final layout of the equation to be obtained is known a priori.

By comparison of (64) with (59) and (62) it appears how the first of them is more suitable for the analysis of the system functioning and for the assessment of the consequences of tampering with its parameters.

V. ANALYSIS OF THE EQUATIONS OF THE WPTS

The analysis of the equations of the WPTS starts from (52), and in particular from its coefficients given by (45) and (48). The impedance $Z_{a,a}$ results from the sum of 4 terms. The first of them is the equivalent impedance of the coil "a" and of its CN. The second and the third terms can be considered as a generalization of (6) and represent the impedance of the loops of coil "b" and of the pickup reflected on the coil "a". Differently from (6), an additional contribution appears in the denominators of both the terms. In the second term it accounts for the impedance of the loop of the pickup reflected on the loop of coil "b" while in the third term it accounts for the impedance of the loop of coil "b" reflected on the loop of the pickup. The last term of (45) has the coefficient 2 because encompasses the two equal contributions of $\bar{V}_{p\to a}$ and $\bar{V}_{b\to a}$, given by (15) and (20), respectively.

As explained in subsection III-A.1, these quantities are the voltages induced by the current $\bar{I}_a$ across its own relevant loop. The first one is the voltage induced across the loop of coil "b", then reflected across the loop of the pickup and, finally, reflected again across the loop of coil "a". The second one is the voltage induced across the loop of the pickup, then reflected across the loop of coil "b" and, finally, reflected back to the loop of coil "a". Even if the order of the reflections is different, the obtained voltages are equal.

Because of the symmetry of the circuit, the three equations (45)-(47) have equal layout and differ only for the values taken by their coefficients. Consequently the analysis carried out for $Z_{a,a}$ holds also for $Z_{b,b}$ and $Z_{ab,p}$.

The gain $K_{b,a}$ accounts for the effect of the supply voltage $\bar{V}_{b,eq}$, applied on the loop of coil "b", on the current $\bar{I}_a$. Thanks to $K_{b,a}$, the coil "a" can be flown by a current $\bar{I}_a \neq 0$ even if $\bar{V}_{a,eq} = 0$, originating a power transfer from coil "b" to coil "a". Following from (53) and (49), the symmetrical consideration holds for $\bar{I}_b$ and $\bar{V}_{a,eq}$ so that the power transfer between the transmitting coils happens also in the reverse direction. Because of the superposition of the effects, the power transfer between the two transmitting coils happens even if both of them are supplied. This effect is mediated by the mutual coupling between the coils in two different ways. The first term in the numerators of (48) and (49) accounts for the direct coupling between coil "a" and coil "b" whilst the second term considers their indirect coupling through the pickup.

The power transfer between coil "a" and coil "b" may be a design choice, such as when coil "b" is used as a "relay" or "resonator" to increase the efficiency of the power transfer between coil "a" and the pickup [22], or could be an unwanted side-effect. In this latter case, (48) and (49) give the obvious hint of reduce as much as possible M_{ab}, i.e. to decouple the transmitting coils. In the same way M_{ap}

TABLE 3. Results computed from equations (both Coils "a" and "b" supplied).

Parameter	Q=∞	Q=300
$Z_{a,a}$	18.0408 - 74.7699i	21.4062 - 73.5272i
$Z_{b,b}$	18.0408 - 74.7699i	21.4668 - 73.7293i
$Z_{ab,p}$	5.6000 - 23.2092i	6.7525 - 23.1832i
$K_{a,b}, K_{b,a}$	-1.0000 - 0.4826i	-0.9836 - 0.5150i
$K_{a,p}$	-0.5571	-0.5565 - 0.0177i
$K_{b,p}$	-0.5571	-0.5566 - 0.0147i

TABLE 4. Results computed from equations (both coils "a" and "b" supplied).

Current	Q=∞	Q=300
$\bar{I}_a$	1.8822∠166.43°	2.0182∠166.35°
$\bar{I}_b$	1.8822∠166.43°	2.0182∠166.35°
$\bar{I}_p$	14.001∠76.43°	13.833∠76.19°

and M_{bp} should be reduced as well, but this approach is unpractical because the power transferred to the pickup would be affected. Instead, analysis of the denominator of (48) and (49) shows that a viable solution to further reduce the power exchanged between the coils consist in adjusting $Z_{a,eq}$, $Z_{b,eq}$, and $Z_{p,eq}$.

From (50), (51) and (54) it comes that if $Z_{a,eq} = Z_{b,eq}$ and $M_{a,p} = M_{b,p}$ the two supply voltages influence $\bar{I}_p$ in the same way. This is a favorable condition because it simplifies the control of the system given that it is sufficient to keep $\bar{V}_{a,eq}$ and $\bar{V}_{b,eq}$ in phase to obtain their maximum combined effect. The requirement of having $Z_{a,eq} = Z_{b,eq}$ can be satisfied, at least at the design stage, by connecting equal CNs to coil "a" and coil "b". On the contrary, the fulfillment of the requirement $M_{a,p} = M_{b,p}$ depends on the actual position of the pickup with respect to the transmitting coils. This position can be different from time to time or, even, it could change during the functioning of the system if a dynamic WPTS is considered. The sensitivity of the WPTS to the difference between $M_{a,p}$ and $M_{b,p}$ can be reduced by designing the CNs so as $Z_{a,eq}$ and $Z_{b,eq}$ are small, as it happens with the series compensation or the LCL compensation of type (c).

VI. ANALYSIS OF A STUDY CASE

The expressions found in Section III and reported in the Appendix have general validity and can be used to analyze the functioning of the WPTS considering the effects of different CNs topologies, coupling conditions, or the presence of parasitic resistances.

In analyzing the study case, the latter ones have been taken in account by the quality factor Q of the inductors and of the capacitors that form the CNs. As a first approximation, Q has been supposed to be equal to the quality factor of the coils' windings, reported in Tab. 2, taken from an available prototype. Consequently, in assigning the values of the impedances of the CNs, a series resistance equal to $\omega L/Q$ has been added to the inductive elements, and a resistance equal to $1/(\omega CQ)$ to the capacitive ones.

It is a common practice to use the series compensation on the pickup in order to maximize the voltage available on the load for a given current in the transmitting coils. Often the series compensation is adopted also for the transmitting coils to decrease the voltage needed to supply them with a given current. Otherwise, the same result can be achieved using the LCL compensation of type (c). As study case, the LCL compensation has been considered both for CN_a and CN_b. The impedances $Z_{a,a}$, $Z_{b,b}$, and $Z_{ab,p}$, and the gains $K_{a,b}$, $K_{a,p}$, $K_{b,a}$, and $K_{b,p}$ have been computed using the inductive parameters listed Tab. 2.

As shown in Tab. 1, this compensation topology is characterized by having $Z_{a,eq} = 0$ and $Z_{b,eq} = 0$, and $Z_{p,eq} = R_L$ in ideal conditions, i.e. if Q= ∞. In this hypothesis, the expressions of the impedances and of the gains given by (45)-(47) and (48)-(51) changes into

$$Z_{a,a} = \frac{\omega^2 M_{ab}^2}{\frac{\omega^2 M_{bp}^2}{Z_{p,eq}}} - 2\frac{j\omega M_{ab} M_{ap}}{M_{bp}} \tag{65}$$

$$Z_{b,b} = \frac{\omega^2 M_{ab}^2}{\frac{\omega^2 M_{ap}^2}{Z_{p,eq}}} - 2\frac{j\omega M_{ab} M_{bp}}{M_{ap}} \tag{66}$$

$$Z_{ab,p} = Z_{p,eq} - 2\frac{j\omega M_{bp} M_{ap}}{M_{ab}} \tag{67}$$

$$K_{a,b} = -\frac{j\omega M_{ab} Z_{p,eq} + \omega^2 M_{bp} M_{ap}}{\omega^2 M_{ap}^2} \tag{68}$$

$$K_{b,a} = -\frac{j\omega M_{ab} Z_{p,eq} + \omega^2 M_{bp} M_{ap}}{\omega^2 M_{bp}^2} \tag{69}$$

$$K_{a,p} = -\frac{M_{bp}}{M_{ab}} \tag{70}$$

$$K_{b,p} = -\frac{M_{ap}}{M_{ab}}. \tag{71}$$

Some of the previous expressions have been obtained as limit values computed for $Z_{a,eq}$ and $Z_{b,eq}$ going to 0.

Analysis of (65)-(68) shows that, despite of having a purely resistive equivalent load and null equivalent impedances of the transmitting coil loops, the impedances $Z_{a,a}$, $Z_{b,b}$, and $Z_{ab,p}$ have reactive components. These components and their sensitivity to the variation of Q are quantified in Tab. 3, obtained mathematically by computing (65)-(71) using the parameters of Tab. 2 and considering Q= ∞ and Q=300. In this latter case $Z_{a,eq}$ and $Z_{b,eq}$ are not exactly equal to 0 because of the parasitic resistances. The amplitude and the phase of the currents $\bar{I}_a$, $\bar{I}_b$, and $\bar{I}_p$, computed by substituting (65)-(71) in (52)-(54) with Q= ∞ and Q=300, are listed in Tab. 4. In both the cases, the sinusoidal supply voltages $\bar{V}_a$ and $\bar{V}_b$, which have an amplitude of 300 V and are in phase each to the other, have been used as phase reference.

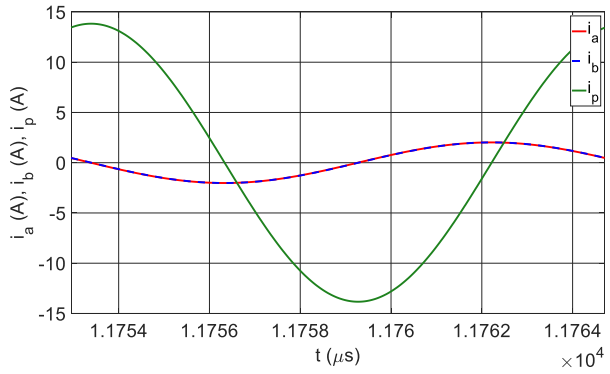

FIGURE 12. Currents in the transmitting coil and in the pickup with both the coils supplied and Q=300.

TABLE 5. Simulation results (both coils "a" and "b" supplied).

Current	Q=10^6	Q=300
$\bar{I}_a$	1.8866∠166.17°	2.0201∠166.36°
$\bar{I}_b$	1.8823∠166.67°	2.0198∠166.05°
$\bar{I}_p$	13.999∠76.42°	13.833∠76.19°

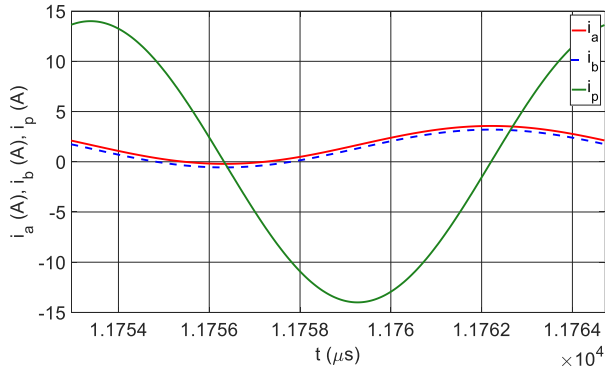

FIGURE 13. Currents in the transmitting coil and in the pickup with both the coils supplied and Q=10^6.

The numerical results of Tab. 4 have been substantiated by means of some simulations performed in the Matlab/Simulink environment implementing the circuit of Fig. 2. Fig. 12 reports the waveforms of the instantaneous current i_a, i_b, and i_p obtained setting Q=300 and relevant to the 1000$^{\text{th}}$ supply period after the system turning on. The plots show that the system reached the steady state and that the amplitudes and the initial phases of the currents, reported in the right column of Tab. 5, agree nearly perfectly with the outcomes of the numerical computation. Fig. 13 shows the same quantities obtained setting $Q = 10^6$. It was not possible to study the system with Q= ∞ because of some convergence problems in the simulation. In this case, because of the high Q, the system has not yet reached the steady state and both i_a and i_b still have a direct component. Despite this difference, the parameters relevant to the alternate component of the currents match very well with those obtained by computation.

TABLE 6. Results computed from equations (only Coil "a" supplied).

Current	Q=∞	Q=300
$\bar{I}_a$	3.9004∠-103.56°	3.9172∠-105.47°
$\bar{I}_b$	4.3308∠102.19°	4.3492∠102.16°
$\bar{I}_p$	7.007∠76.43°	6.9174∠76.34°

TABLE 7. Simulation results (only Coil "a" supplied).

Current	Q=∞	Q=300
$\bar{I}_a$	3.8453∠-103.65°	3.9175∠-105.48°
$\bar{I}_b$	4.2884∠102.44°	4.3493∠102.17°
$\bar{I}_p$	6.9921∠76.40°	6.9168∠76.34°

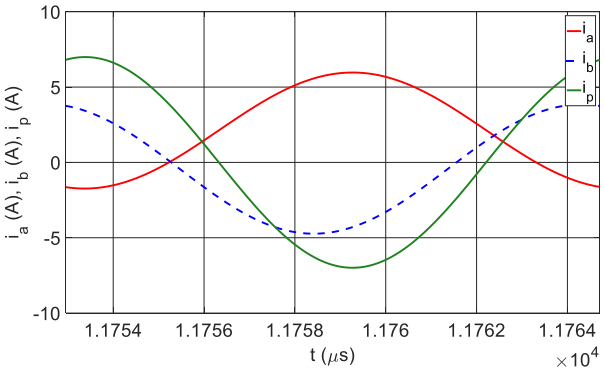

FIGURE 14. Currents in the transmitting coil and in the pickup with only coil "a" supplied and Q=10^6.

Equations (65)-(71) can be used also to study the effect of the mutual coupling between the transmitting coils. To this end, it is enough to set, for example, $\bar{V}_{b,eq} = 0$ and to compute again (52)-(54). With this arrangement, the amplitude and the phase of the currents with $Q = \infty$ and $Q = 300$ take the values listed in Tab. 6. The corresponding quantities coming from the simulations are reported in Tab. 7 whilst Fig. 14 shows the waveforms of the currents obtained with $Q = 10^6$. Also in this case, nor i_a neither i_b reach the steady state at the end of the 1000$^{\text{th}}$ supply period, nevertheless the simulation results relevant to their alternate component match very well with the computed ones.

In some WPT applications the transmitting coils are decoupled by means of suitable solutions [23], [24]. Ideally, this arrangement forces M_{ab} =0, but in this condition (65)-(71) give meaningless results. The physical reason of this behavior is that, being $Z_{a,eq} = Z_{b,eq}$ =0, from the scheme of Fig. 7a it derives that both the supply voltage $\bar{V}_{a,eq}$ and $\bar{V}_{b,eq}$ should be equal to the voltages induced by $\bar{I}_p$ across coil "a" and coil "b". Given that $\bar{V}_{a,eq}$ and $\bar{V}_{b,eq}$ are the inputs of the system, this condition is not met unless they have the same value by hypothesis.

$$\bar{V}_{a,eq} = \left(Z_{a,eq} + \frac{\omega^2 M_{ab}^2}{Z_{b,eq} + \frac{\omega^2 M_{bp}^2}{Z_{p,eq}}} + \frac{\omega^2 M_{ap}^2}{Z_{p,eq} + \frac{\omega^2 M_{bp}^2}{Z_{b,eq}}} - 2\frac{j\omega^3 M_{ab} M_{bp} M_{ap}}{Z_{p,eq} Z_{b,eq} + \omega^2 M_{bp}^2} \right) \bar{I}_a \tag{A1}$$

$$\bar{V}_{a,eq} \left(-\frac{j\omega M_{ab} Z_{p,eq} + \omega^2 M_{bp} M_{ap}}{Z_{p,eq} Z_{a,eq} + \omega^2 M_{ap}^2} \right) = \left(Z_{b,eq} + \frac{\omega^2 M_{ab}^2}{Z_{a,eq} + \frac{\omega^2 M_{ap}^2}{Z_{p,eq}}} + \frac{\omega^2 M_{bp}^2}{Z_{p,eq} + \frac{\omega^2 M_{ap}^2}{Z_{a,eq}}} - 2\frac{j\omega^3 M_{ab} M_{bp} M_{ap}}{Z_{p,eq} Z_{a,eq} + \omega^2 M_{ap}^2} \right) \bar{I}_b \tag{A2}$$

$$\bar{V}_{a,eq} \left(-\frac{j\omega M_{ap} Z_{b,eq} + \omega^2 M_{bp} M_{ab}}{Z_{a,eq} Z_{b,eq} + \omega^2 M_{ab}^2} \right) = \left(Z_{p,eq} + \frac{\omega^2 M_{ap}^2}{Z_{a,eq} + \frac{\omega^2 M_{ab}^2}{Z_{b,eq}}} + \frac{\omega^2 M_{bp}^2}{Z_{b,eq} + \frac{\omega^2 M_{ab}^2}{Z_{a,eq}}} - 2\frac{j\omega^3 M_{ab} M_{bp} M_{ap}}{Z_{a,eq} Z_{b,eq} + \omega^2 M_{ab}^2} \right) \bar{I}_p \tag{A3}$$

$$\bar{V}_{b,eq} = \left(Z_{b,eq} + \frac{\omega^2 M_{ab}^2}{Z_{a,eq} + \frac{\omega^2 M_{ap}^2}{Z_{p,eq}}} + \frac{\omega^2 M_{bp}^2}{Z_{p,eq} + \frac{\omega^2 M_{ap}^2}{Z_{a,eq}}} - 2\frac{j\omega^3 M_{ab} M_{bp} M_{ap}}{Z_{p,eq} Z_{a,eq} + \omega^2 M_{ap}^2} \right) \bar{I}_b \tag{A4}$$

$$\bar{V}_{b,eq} \left(-\frac{j\omega M_{ab} Z_{p,eq} + \omega^2 M_{bp} M_{ap}}{Z_{p,eq} Z_{b,eq} + \omega^2 M_{bp}^2} \right) = \left(Z_{a,eq} + \frac{\omega^2 M_{ab}^2}{Z_{b,eq} + \frac{\omega^2 M_{bp}^2}{Z_{p,eq}}} + \frac{\omega^2 M_{ap}^2}{Z_{p,eq} + \frac{\omega^2 M_{bp}^2}{Z_{b,eq}}} - 2\frac{j\omega^3 M_{ab} M_{bp} M_{ap}}{Z_{p,eq} Z_{b,eq} + \omega^2 M_{bp}^2} \right) \bar{I}_a \tag{A5}$$

$$\bar{V}_{b,eq} \left(-\frac{j\omega M_{bp} Z_{a,eq} + \omega^2 M_{ap} M_{ab}}{Z_{a,eq} Z_{b,eq} + \omega^2 M_{ab}^2} \right) = \left(Z_{p,eq} + \frac{\omega^2 M_{ap}^2}{Z_{a,eq} + \frac{\omega^2 M_{ab}^2}{Z_{b,eq}}} + \frac{\omega^2 M_{bp}^2}{Z_{b,eq} + \frac{\omega^2 M_{ab}^2}{Z_{a,eq}}} - 2\frac{j\omega^3 M_{ab} M_{bp} M_{ap}}{Z_{a,eq} Z_{b,eq} + \omega^2 M_{ab}^2} \right) \bar{I}_p \tag{A6}$$

VII. CONCLUSION

This paper presented a new approach to work out the equations that describe the functioning of the compensation networks of a WPTS. The obtained equations are equivalent to those achieved using the conventional methods for the circuital analysis, but are written with a layout that allows to recognize at a first glance the contribution of the different CNs and of the coil couplings. A qualitative analysis of the WPTS functioning has been performed by inspection of the obtained equations. A WPTS with series and LCL compensation has been used as case study for the numerical implementation of the equations. The obtained results have been confirmed by comparison with the outcoming of circuital simulations.

APPENDIX

The expressions that link the currents in the transmitting coils and in the pickup to the supply voltages (A1)–(A6), as show at the top of the page.

REFERENCES

[1] M. Ehsani, Y. Gao, and A. Emadi, *Modern Electric, Hybrid Electric, and Fuel Cell Vehicles: Fundamentals, Theory, and Design*, 2nd ed. Boca Raton, FL, USA: CRC Press, 2010, doi: 10.1201/9781420054002.

[2] J. Larminie and J. Lowry, *Electric Vehicle Technology Explained*, 2nd ed. Hoboken, NJ, USA: Wiley, 2012, doi: 10.1002/9781118361146.

[3] M. Yilmaz and P. T. Krein, "Review of battery charger topologies, charging power levels, and infrastructure for plug-in electric and hybrid vehicles," *IEEE Trans. Power Electron.*, vol. 28, no. 5, pp. 2151–2169, May 2013, doi: 10.1109/TPEL.2012.2212917.

[4] M. Eghtesadi, "Inductive power transfer to an electric vehicle-analytical model," in *Proc. 40th IEEE Conf. Veh. Technol.*, Orlando, FL, USA, 1990, pp. 100–104, doi: 10.1109/vetec.1990.110303.

[5] S. Li and C. C. Mi, "Wireless power transfer for electric vehicle applications," *IEEE J. Emerg. Sel. Topics Power Electron.*, vol. 3, no. 1, pp. 4–17, Mar. 2015, doi: 10.1109/JESTPE.2014.2319453.

[6] G. A. Covic and J. T. Boys, "Modern trends in inductive power transfer for transportation applications," *IEEE J. Emerg. Sel. Topics Power Electron.*, vol. 1, no. 1, pp. 28–41, Mar. 2013, doi: 10.1109/JESTPE.2013.2264473.

[7] H. Feng, R. Tavakoli, O. C. Onar, and Z. Pantic, "Advances in high-power wireless charging systems: Overview and design considerations," *IEEE Trans. Transport. Electrific.*, vol. 6, no. 3, pp. 886–919, Sep. 2020, doi: 10.1109/TTE.2020.3012543.

[8] W. Zhang, J. C. White, A. M. Abraham, and C. C. Mi, "Loosely coupled transformer structure and interoperability study for EV wireless charging systems," *IEEE Trans. Power Electron.*, vol. 30, no. 11, pp. 6356–6367, Nov. 2015, doi: 10.1109/TPEL.2015.2433678.

[9] A. Kurs, A. Karalis, R. Moffatt, J. D. Joannopoulos, P. Fisher, and M. Soljačić, "Wireless power transfer via strongly coupled magnetic resonances," *Science*, vol. 317, no. 5834, pp. 83–86, Jul. 2007, doi: 10.1126/science.1143254.

[10] T. C. Beh, M. Kato, T. Imura, S. Oh, and Y. Hori, "Automated impedance matching system for robust wireless power transfer via magnetic resonance coupling," *IEEE Trans. Ind. Electron.*, vol. 60, no. 9, pp. 3689–3698, Sep. 2013, doi: 10.1109/TIE.2012.2206337.

[11] C.-S. Wang, O. H. Stielau, and G. A. Covic, "Design considerations for a contactless electric vehicle battery charger," *IEEE Trans. Ind. Electron.*, vol. 52, no. 5, pp. 1308–1314, Oct. 2005, doi: 10.1109/TIE.2005.855672.

[12] J. Sallan, J. L. Villa, A. Llombart, and J. F. Sanz, "Optimal design of ICPT systems applied to electric vehicle battery charge," *IEEE Trans. Ind. Electron.*, vol. 56, no. 6, pp. 2140–2149, Jun. 2009, doi: 10.1109/TIE.2009.2015359.

[13] *Wireless Power Transfer for Light-Duty Plug-in/Electric Vehicles and Alignment Methodology*, Standard J2954, SAE International, Warrendale, PA, USA, 2020.

[14] S. Chopra and P. Bauer, "Analysis and design considerations for a contactless power transfer system," in *Proc. IEEE 33rd Int. Telecommun. Energy Conf. (INTELEC)*, Amsterdam, The Netherlands, Oct. 2011, pp. 1–6, doi: 10.1109/INTLEC.2011.6099774.

[15] A. Sagar, A. Kumar, M. Bertoluzzo, and R. K. Jha, "Analysis and design of a two-winding wireless power transfer system with higher system efficiency and maximum load power," in *Proc. 48th Annu. Conf. IEEE Ind. Electron. Soc.*, Brussels, Belgium, Oct. 2022, pp. 1–6, doi: 10.1109/IECON49645.2022.9968858.

[16] C. Zheng, R. Chen, E. Faraci, Z. U. Zahid, M. Senesky, D. Anderson, J.-S. Lai, W. Yu, and C.-Y. Lin, "High efficiency contactless power transfer system for electric vehicle battery charging," in *Proc. IEEE Energy Convers. Congr. Expo.*, Denver, CO, USA, Sep. 2013, pp. 3243–3249, doi: 10.1109/ECCE.2013.6647126.

[17] D.-H. Tran, V.-B. Vu, V.-L. Pham, and W. Choi, "Design and implementation of high efficiency wireless power transfer system for on-board charger of electric vehicle," in *Proc. IEEE 8th Int. Power Electron. Motion Control Conf.*, Hefei, China, May 2016, pp. 2466–2469, doi: 10.1109/IPEMC.2016.7512685.

[18] Q. Zhu, L. Wang, and C. Liao, "Compensate capacitor optimization for kilowatt-level magnetically resonant wireless charging system," *IEEE Trans. Ind. Electron.*, vol. 61, no. 12, pp. 6758–6768, Dec. 2014, doi: 10.1109/TIE.2014.2321349.

[19] F. F. Judd and P. M. Chirlian, "The application of the compensation theorem in the proof of Thevenin's and Norton's theorems," *IEEE Trans. Educ.*, vol. E-13, no. 2, pp. 87–88, Aug. 1970, doi: 10.1109/TE.1970.4320572.

[20] G. E. Chatzarakis, M. D. Tortoreli, and A. D. Tziolas, "Thevenin and Norton's theorems: Powerful pedagogical tools for treating special cases of electric circuits," *Int. J. Electr. Eng. Educ.*, vol. 40, no. 4, pp. 299–314, Oct. 2003, doi: 10.7227/ijeee.40.4.6.

[21] M. F. Moad, "On Thevenin's and Norton's equivalent circuits," *IEEE Trans. Educ.*, vol. E-25, no. 3, pp. 99–102, Aug. 1982, doi: 10.1109/TE.1982.4321556.

[22] T. Maruyama, T. Kimura, and M. Nakatsugawa, "Magnetic coupling WPT efficiency improvement by inserting relay coil with optimized load impedance," in *Proc. IEEE Int. Symp. Antennas Propag. USNC-URSI Radio Sci. Meeting (APS/URSI)*, Singapore, Dec. 2021, pp. 455–456, doi: 10.1109/APS/URSI47566.2021.9704802.

[23] A. Zaheer, H. Hao, G. A. Covic, and D. Kacprzak, "Investigation of multiple decoupled coil primary pad topologies in lumped IPT systems for interoperable electric vehicle charging," *IEEE Trans. Power Electron.*, vol. 30, no. 4, pp. 1937–1955, Apr. 2015, doi: 10.1109/TPEL.2014.2329693.

[24] W. Chen, H. Li, and W. Lu, "Decoupling design of multi-coil wireless power transfer system with metal insulator," in *Proc. IEEE PELS Workshop Emerg. Technol., Wireless Power Transf. (WoW)*, Chongqing, China, May 2017, pp. 30–33, doi: 10.1109/WoW.2017.7959360.

MANUELE BERTOLUZZO received the M.S. degree in electronic engineering from the University of Padua, Padua, Italy, in 1993, and the Ph.D. degree in industrial electronics and computer science, in 1997.

Since 2015, he has been an Associate Professor with the Department of Industrial Engineering, University of Padua. He holds the lectureship of road electric vehicles and systems for automation. He is involved in analysis and design of power electronics systems, especially for wireless charging of electric vehicles battery.

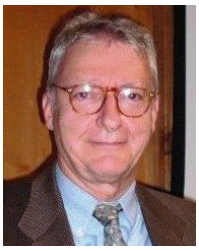

GIUSEPPE BUJA (Life Fellow, IEEE) received the Laurea degree (Hons.) in power electronics engineering from the University of Padua, Padua, Italy.

He is currently a Senior Research Scientist with the University of Padua. He has carried out an extensive research work in the field of power and industrial electronics, originating the modulating-wave distortion, and the optimum modulation for pulse-width modulation inverters. His current research interests include automotive electrification, including the wireless charging of electric vehicles and the grid-integration of renewable energies.

DANIELE DESIDERI is currently an Associate Professor in electrical engineering with the University of Padua. He is the coauthor in about 90 papers, published in journals or proceedings of international conferences, in the fields of plasma and thermonuclear fusion engineering, electromagnetic compatibility, and nanostructured films. His current research interests include piezoelectric devices and wireless power transfer.

AMRITANSH SAGAR (Senior Member, IEEE) was born in Saharsa, India. He received the B.Tech. degree in electrical and electronics engineering from the Birla Institute of Technology, Mesra, Jharkhand, India, in 2011, and the M.Tech. degree in power electronics and drives from the Sardar Vallabhbhai National Institute of Technology, Surat, India, in 2017. He is currently pursuing the Ph.D. degree with the Department of Industrial Engineering, University of Padua, Padua, Italy.

He joined the University of Padua, in October, 2020. From August 2017 to December 2018, he was an Assistant Professor with Silver Oak University, Ahmedabad, and from March 2019 to June 2020, he was a Junior Research Fellow with VIT, Vellore, India. His research interests include the wireless power transfer, modeling, design, and control of power.

Open Access funding provided by 'Università degli Studi di Padova' within the CRUI CARE Agreement